Research Square

Preprints are preliminary reports that have not undergone peer review.
They should not be considered conclusive, used to inform clinical practice,
or referenced by the media as validated information.

Anti-inflammatory and anti-oxidant activities of Gymnema sylvestre extract rescues acute respiratory distress syndrome in rats via modulating the NF-κB/MAPK pathway

ARUNA JANGAM
IICT CSIR: Indian Institute of Chemical Technology
SATYA KRISHNA TIRUNAVALLI
IICT CSIR: Indian Institute of Chemical Technology
BALA MANIKANTHA ADIMOOLAM
IICT CSIR: Indian Institute of Chemical Technology
BHAVANA KASIREDDY
IICT CSIR: Indian Institute of Chemical Technology
SAMATA SAI PATNAIK
IICT CSIR: Indian Institute of Chemical Technology
Jayashankar Erukkambattu
AIIMS: All India Institute of Medical Sciences
Jagadeshwar Reddy Thota
IICT CSIR: Indian Institute of Chemical Technology
Sai Balaji Andugulapati
IICT CSIR: Indian Institute of Chemical Technology
ANTHONY ADDLAGATTA (anthony@iict.res.in)
IICT CSIR: Indian Institute of Chemical Technology https://orcid.org/0000-0003-4666-9327

Research Article

Keywords: Acute respiratory distress syndrome, cytokine-storm, lung injury, phytochemicals, Gymnema sylvestre, gymnemic acid, neutrophil-elastase

Posted Date: July 20th, 2022

DOI: https://doi.org/10.21203/rs.3.rs-1841071/v1

License: This work is licensed under a Creative Commons Attribution 4.0 International License.
Read Full License

Version of Record: A version of this preprint was published at Inflammopharmacology on January 20th, 2023. See the published version at https://doi.org/10.1007/s10787-022-01133-5.

Abstract

Acute respiratory distress syndrome (ARDS) is one of the major cause of mortality in COVID-19 patients, due to limited therapeutic options. This prompted us to explore natural sources to mitigate this condition. Gymnema sylvestre (GS) is an ancient medicinal plant known to have various therapeutic effects. In this investigation, Gymnema sylvestre hydroalcoholic extract (HAEGS) was examined against lipopolysaccharide (LPS) induced lung injury and ARDS in *in vitro* and *in vivo* models. UHPLC-HRMS/GC-MS was employed for characterizing the HAEGS and identified several active derivatives including gymnemic acid, gymnemasaponins, gymnemoside, gymnemasin, quercetin, and long fatty acids. Gene expression by RTqPCR and DCFDA analysis by flow-cytometry revealed that several inflammatory cytokine/chemokine, cell injury markers, and reactive-oxygen-species (ROS) levels were highly upregulated in LPS control and were significantly reduced upon HAEGS treatment. Consistent with the in vitro studies, we found that in LPS induced ARDS model, pre-treatment with HAEGS significantly suppressed the LPS-induced elevation of inflammatory cell infiltrations, cytokine/chemokine marker expression, ROS levels, and lung injury in a dose dependent manner. Further mechanistic studies suggested that the HAEGS ameliorates the ARDS through the NF-κB/MAPK signaling pathway. Additional fractionation results revealed that fraction-6 which has the exclusive composition of gymnemic acid derivatives showed anti-inflammatory effects which is similar to the HAEGS. Overall, HAEGS significantly mitigated the LPS-induced lung injury and ARDS by targeting NF-κB/MAPK signaling pathway. Thus, our work unravels the protective role of HAEGS for the first time in managing ARDS.

1.0 Introduction

Inflammation-mediated lung diseases are a major cause of morbidity/mortality in COVID-19 patients who were admitted to intensive care units (Merad & Martin, 2020). Pathogenic infections induce hyperactivation of immune cells leading to cytokine release syndrome (CRS), which is a hallmark of ARDS. Cytokine storm is the main cause of death in the Covid-19 patients (Spagnolo et al., 2020). To the best of our knowledge there is no specific drug to treat the ARDS except for few antibodies that target specific cytokines. The available data are inadequate to conclude the therapeutic effect of IL-6 antibodies (Tocilizumab) in the ARDS (Khiali, Khani, & Entezari-Maleki, 2020). Cytokines are small secreted proteins, which are produced by nearly every cell to regulate and influence immune response (Takeuchi & Akira, 2010). IL-6 and other pro-inflammatory cytokines (TNFα, IFNγ, IL-10, IL-1β, IL-12p40, IL-17A, IL-2, MIP1α, and IL-8) involve the inflammatory cascade and contribute to host defense against infections. Inflammatory chemokines such as CCL-2, CCL-7, and CXCL-1) acts as a chemoattractant for leukocytes, recruiting monocytes, neutrophils, and other effector cells and initiate the infiltration of inflammatory cells from the blood to sites of infection or the target organ. In addition to inflammatory cells, respiratory epithelium or lung epithelial cells are also involved in maintaining the integrity of the lungs, their function, and host responses to pathogenesis and resolution of ALI/ARDS upon infections (Manicone, 2009). Despite the advances in ventilator and intensive care therapies with novel drugs, the mortality rate remains high and it exceeds 50% in ARDS patients (Aslan, Aslan, Zolbanin, & Jafari, 2021). Due to the

lack of first-line treatment for ARDS, glucocorticoids are being used as an anti-inflammatory and immunosuppressive agent and their outcomes are not proved to be beneficial (Barnes & Adcock, 1993).

Gymnema sylvestre (GS), is a phytopharmaceutical used in Ayurveda to treat diabetes and various inflammatory diseases (Baskaran, Kizar Ahamath, Radha Shanmugasundaram, & Shanmugasundaram, 1990; Pragya Tiwari, B. N. Mishra, & Neelam S. Sangwan, 2014). GS belongs to Asclepiadaceae family and is found in tropical forests of India, Africa and Australia (Parijat Kanetkar, Rekha Singhal, & Madhusudan Kamat, 2007). Main constituents of GS include gymnemic acids, which are triterpenoid saponins responsible for antidiabetic activity (Leach, 2007). In addition to gymnemic acids, GS contains alkaloids, anthraquinones, chlorophylls, flavones, quercitol etc that mitigate the inflammatory markers. An extract of GS significantly reduced the paw oedema volume by 48% and inhibited the formation of granuloma at 300 mg/kg when compared with the control group (Malik, Manvi, Alagawadi, & Noolvi, 2008). Ethanol extract of GS is known to reduce the blood sugar and lipid levels in various animals models (P. Tiwari, B. N. Mishra, & N. S. Sangwan, 2014). The blood glucose lowering effects GS extracts is due to the inhibition of T1R2+T1R3 sweet receptors by gymnemic acid and its derivatives there by reducing the glucose absorption (P. Kanetkar, R. Singhal, & M. Kamat, 2007; Sahu, Mahato, Sarkar, & Poddar, 1996). In a different study, hydroalcoholic extracts also mitigated the ulcerative colitis in Wistar albino rats by suppressing the oxidative and inflammatory response, and protected colonic mucosal content (Aleisa et al., 2014). These beneficial effects were achieved by reducing the level of pro-inflammatory cytokines like IL-1β, IL-6 and TNF-α in the colon tissue. Other components like quercetin also exhibit strong antioxidant and anti-inflammatory activity against various disease models (Yao Li et al., 2016). It has been established that gymnemic acid alleviates inflammation and insulin resistance in db/db mice via PPARδ- and NFκB-mediated pathways (Y. Li et al., 2019). Recent simulation studies on bioactive molecules of GS, revealed that gymnemic acid as a ligand binding with a 3CLpro as a COVID-19 therapeutic target (Subramani, Gupta, Manish, & Prasad, 2020). Together, these studies have prompted us to evaluate the protective nature of the hydroalcoholic extract GS (HAEGS) against LPS induced *in-vitro* and *in-vivo* ARDS models. We further separated various components on column chromatography and identified a specific fraction that mimicked the anti-inflammatory properties of the whole hydroalcoholic extract. Systematic chemical characterization established the chemical composition of the extract. By adopting various biochemical tools, we established the possible mechanism for the therapeutic activity of HAEGS.

2.0 Experimental Methodology

2.1. Materials

Lipopolysaccharide (LPS) from E. coli 055: B5, LC-MS and HPLC grade solvents and fine chemicals were procured from Sigma Aldrich, USA. SYBR green mix cDNA synthesis kit and were purchased from Takara Bioscience, India. ELISA kits (IL-6, CCL2, INF-γ and IL-1β) were obtained from R&D Systems. Primary antibodies were purchased from Cell Signalling Technology, USA and corresponding catalogue numbers and are mentioned in supplementary table S2. Bicinchoninic acid reagent (BCA-kit) was bought from

Thermo scientific, USA. Polyvinylidene difluoride (PVDF) membrane (0.45 µm) was procured from Millipore, USA. Secondary antibodies were procured from Jackson Laboratory, USA and an ECL kit was purchased from Advansta, Menlo Park, CA, USA. Deionized water (18 MΩ) was used for preparation of all solutions. Leaves of G. Sylvestre were collected from Chittoor district, Andhra Pradesh, India. The plant specimen was authenticated by a botany professor from Osmania University, Hyderabad, India. LC-MS CHROMASOLVs grade and HPLC grade methanol (MeOH) and acetonitrile (ACN) were procured from Sigma-Aldrich (Bangalore, India). Analytical reagent (AR) grade ammonium acetate, ammonium formate, formic acid, hydrochloric acid (HCl).

2.2 Cell lines and culture conditions

RAW-264.7 cell line (murine macrophages) was procured from ATCC and cultured in DMEM (Dulbecco's modified Eagle's) medium with 1.5 g/litre sodium bicarbonate, 4 mM L-glutamine, 4.5 g/litre glucose, and 10% FBS (fetal bovine serum). Human bronchial epithelial cell line (BEAS-2B cell-line) was purchased from Lonza, USA and cultured using BEGM media with growth factors. Both the cell lines were cultured in a 5% CO_2 incubator with humidified atmosphere of 95% air at 37 °C. All cell lines were used in between 4-5 passages.

2.3 Preparation of hydroalcoholic extract of the *Gymnema sylvestre* (HAEGS)

The shade dried leaves of Gymnema sylvestre were powdered and employed hydroalcoholic maceration method for extracting the hydroalcoholic GS extract. The coarse powder (639 grams) of Gymnema sylvestre was added into the mixture of 5.62L of ethanol and 1.87L of water (in 3:1 ratio) in a beaker with constant stirring using magnetic stirrers for a period of 48 hr at 25 °C. Extracted solution was filtered through a muslin cloth and evaporated to dryness using rotary evaporator at temperature below 55 °C under vacuum. The dried powder of HAEGS was stored at 4 °C in colored glass bottles until further use.

2.3.1 Fractionation of HAEGS

Part of the crude extract (HAEGS) was dissolved in acetone:chloroform solvent mixture and loaded onto silica column (Fig. S8A). For separating various compounds, a mixture of acetone:hexane (shown in scheme.1), mixture of methanol: chloroform in various ratios, and lastly methanol solvents were used. By increasing the polarity, 30 fractions were collected in total, and the fractions with similar thin layer chromatography (TLC) patterns (Fig. S8B) were mixed together to afford six major fractions (F1-F6). Fraction 31 (labelled as F7) obtained with methanol elution did not provide any detectable organic molecules and hence it was discarded.

2.4 Phytochemical profiling of HAEGS extract

2.4.1 Sample preparation

The samples were dissolved in methanol, centrifuged and filtered using a 0.22 µm membrane filter and final concentrations of crude samples were injecting (1µL) into the UHPLC/Thermo OrbitrapExactive

mass spectrometer (Thermo Scientific, Bremen, Germany) system.

2.4.2 Development and optimization of chromatographic conditions:

Analytical separations of HAEGS were achieved on a Surveyor UHPLC system (Thermo Scientific, Germany) consisting a quaternary gradient pump, an auto-injector and an in-line degasser. The column compartment maintained at a temperature of 25°C. The chromatographic separation method was developed in reverse phase mode with Syncronis C18 column (2.1 × 100mm;Thermo scientific, Germany) (Dadinaboyina et al., 2021). Varying the selectivity determination factors such as pH of mobile phase, ratios of polarity change and flow rate optimized the method. Finally, acceptable separation was achieved using 0.1% formic acid in water (A) and acetonitrile (ACN) (B) with a flow rate of 0.15 mL min^{-1} in gradient elution mode. The following linear gradient elution was used:(Time in min/%B); 0-1/5, 1-12/5, 12-16/95, 19-21/95, and 21-26/5. The column was equilibrated with 20 column volumes of mobile phase at the composition prior to sample injection and the injection volume was 1µl.

2.4.3 Mass spectrometry

Mass spectral analysis was carried out on Thermo Orbitrap Exactive mass spectrometer (Thermo Scientific, Bremen, Germany). The eluent from the UHPLC system was directed into the mass spectrometer via heated electrospray ionization (HESI) interface and operated in the positive& negative ion mode. The mass spectrometer was calibrated before analysis using the manufacturer's calibration solution (ProteoMass LTQ/FN-Hybrid ESI Pos. Mode Cal Mix, SUPELCO) to obtain the mass range in external calibration mode. Parameters of the ion source were as follows: positive ion spray voltage 3.50 kV, negative ion spray voltage 2.50 kV, heater temperature 275 °C, capillary temperature 320 °C, capillary voltage 67.50 V, tube lens voltage 140 V, skimmer voltage 20 V, sheath gas flow 30 (arbitrary units), auxiliary gas flow 15 (arbitrary units) and sweep gas 0 (arbitrary units). Nitrogen was used as the sheath and auxiliary gas in the ion source. The instrument was operated in full scan and automatic MS/MS experiments over the range 100-2000 m/z at a resolving power of 100,000 (full width at half maximum) using nitrogen as collision gas.

2.4.4 GC-MS analysis

The GC analysis was performed using Agilent 6890 GC equipped with Agilent Technologies 5977A mass selective detector (MSD). The separation of analytes was carried out on capillary column (Agilent) HP-5 5% Phenyl Methyl Siloxane (30mx250umx0.5um). The injection port temperature was maintained at 240°C and the oven was programmed from 50°C to 280°C at a ramp rate of 10°C/min with initial hold up temperature time as 2 minutes and the final hold up temperature time as 5 minutes. Helium was used as a carrier gas at a flow rate of 1.2 mL/min. The desorption of analytes and injection into the column was carried out in splitless mode to avoid the loss of low abundant volatiles. GC-MS interface, ion source and quadrupole temperatures were maintained at 280°C, 230°C, and 150°C respectively. The ionization of volatiles was carried out in electron ionization source at 70 eV electron energy, and the scan range was

fixed at 30 - 800 units. The volatile organic compounds were identified by using the W9N11.L, NIST14 library database. Mass spectral data was processed using MSD Chem Station.

2.5 *In-vitro* assays

2.5.1 Treatment conditions for *in-vitro* experiments

Macrophage (RAW-264.7) cells were seeded in 24 well plate ($0.5x10^5$/well) for estimating the IL-6 levels using ELISA. For all other cell culture experiments, RAW-264.7 or BEAS-2B cells were seeded in 6 well plate ($3 x10^5$/well) and incubated for 18 hr, then cells were washed with phosphate buffer saline (1xPBS) and cultured with serum-free media for another 6 hr. Further, cells were pre-treated with HAEGS (125, 250 and 500 µg/mL), different fractions or Indomethacin (50 and 100 µM) or Dexamethasone (100 and 500 ng/mL) for 2 hr, then cells were activated with LPS (1 µg/mL for RAW-264.7 and 5 µg/mL for BEAS-2B cells) and incubated for 12 hr. Then, cell supernatant was collected for nitric oxide estimation and ELISA while cells were harvested for gene expression and Western-blot analysis.

2.5.2 Cell viability by SRB assay

Sulphorodamine-B (SRB) assay was performed for assessing the cell viability as published previously (S. K. Tirunavalli et al., 2021). Briefly, $5x10^3$ cells/well were seeded in a 96 well plate, then cells were treated with sterile water (vehicle control) or HAEGS at various concentrations (125, 250 and 500 µg/mL) in presence or absence of LPS. After 48 hr, SRB assay was performed. IC_{50} values were calculated using curve-fit method by GraphPad Prism-5.

2.5.3 Gene expression analysis

After treatment period, treated cells or rat lung tissues were subjected to RNA isolation using RNAiso plus as described earlier (Andugulapati, Gourishetti, Tirunavalli, Shaikh, & Sistla, 2020). Briefly, RNA was isolated using the trizol-chloroform method and total RNA was quantified using nano-drop. Isolated RNA (1µg) was subjected to cDNA synthesis using prime script cDNA synthesis kit as per the manufacturer's instructions. Specified primers [*IL-6, IL-1β, TNF-α, IL-8, CCL2, CCL3, CCL7, CXCL1*, alveolar pulmonary stretch (amphiregulin), *CC16*, vascular cell adhesion molecule-1 (*VCAM-1*), intercellular adhesion molecule *(ICAM-1)*, and reference markers *(GAPDH, β2M, and β-actin)]* were designed using Primer-3 software and respective sequences are shown in Table S1. RT-qPCR was carried out using SYBR green mix and the differences in mRNA expression of the specified genes were calculated as the fold change using the formula $2^{-\Delta\Delta ct}$ and data was expressed as Mean ±SEM.

2.5.4 ROS measurement using DCFDA assay

ROS estimation was performed using DCFDA staining as described earlier (Satya Krishna Tirunavalli et al., 2021). Briefly, after pre-treating the cells with specified concentrations of HAEGS for 2 hr, cells were

activated with LPS for another 12 hr. Then DCFDA assay was performed using BD-Accuri® C6 flow cytometer for mean florescence intensity of DFCDA.

2.5.5 Immunoblotting analysis

Cells or rat lung tissues that were treated by HAEGS followed by LPS stimulation were subjected to Western-blot analysis as described earlier (Andugulapati et al., 2020). Briefly, cells or tissue samples were lysed using RIPA lysis buffer and then, protein concentrations were estimated using BCA-kit, then 30 µg of protein per sample was loaded onto the SDS-PAGE Bis-Tris 8–12% protein gel for electrophoresis and then transferred onto PVDF membranes. Further, PVDF membrane was blocked with 5% BSA (Sigma Aldrich, USA) for 1 hr at room temperature followed by incubation with primary antibodies overnight at 4 °C. Then respective secondary antibodies were added and then blots were developed using an ECL kit.

2.6 *In-vivo* Experiments

2.6.1 Induction of ARDS using intra-tracheal instillation of LPS

Adult SD (male) rats weighing 210–240g, (n=32) were used for developing the LPS induced ARDS. As per the Committee for the Purpose of Control and Supervision on Experiments on Animals (CPCSEA) regulations, all the animals were acclimatized at specified temperature (24–26 °C) with maintenance of 12 hr dark and 12 hr light cycles. The experimental protocol was approved by Institutional Animal Ethics Committee (IAEC) (IICT/023/2020), CSIR-Indian Institute of Chemical Technology 6). Male SD rats were randomly assigned to 4 groups (n=8/group). Before LPS administration, rats were pre-treated with HAEGS 125 mg/kg and 250 mg/kg in group 3 and group 4 of the animals respectively. LPS was dissolved in PBS to attain the concentration of 5 mg/mL. All animals were anesthetized with ketamine (80 mg/kg) and xylazine (10 mg/kg). After 12 hr of the pre-treatment, rats were challenged with LPS (5 mg/kg) intratracheally, in treatment groups (group 3 and 4) and LPS control group (group 2). Group 1 of rats were used as a sham control, where PBS was instilled into the rat's trachea while the remaining three groups were used to establish the ARDS model. After 12 hr of LPS administration, rats were again dosed with HAEGS and monitored for further 12 hr. After 24 hr of the LPS stimulation, Bronchoalveolar lavage Fluid (BALF) samples were collected from 50% of the animals from each group and one part of BALF samples were subjected to neutrophil count and, remaining BALF sample was centrifuged and stored in -80 freezer for ELISA. All animals were sacrificed and left lungs were isolated and collected in buffered formalin and subjected to histopathological examination, while the two lobes of the right lungs were collected for wet-to-dry (W/D) analysis and rest of the two lobes were collected for Western blotting, reverse transcription-quantitative PCR (RT-qPCR), ELISA and Nitric oxide examinations.

2.6.2 Lung wet-dry weight (W/D) ratio

After sacrificing animals, one of the right lung tissues was isolated, rinsed with 1XPBS, then the surface liquid of the lobe was removed by draining with clean filter paper, and then wet weight was recorded. Then these lung tissues were incubated in a thermostatic oven at a constant 80°C for 48 hr following by

measuring the dry weight. The W/D ratio was estimated to measure the moisture content in the lung tissues.

2.6.3 BALF analysis

Animals were anesthetized with Pentobarbital 50 mg/kg and then, BALF was collected after exposing the trachea, then trachea was cannulated, and a volume of 3 ml sterile saline was slowly infused into the lungs and collected 2mL of BALF. BALF cell pellet was collected by centrifuging the BALF at 1800 rpm at 4 °C for 12 min, then cell pellet was re-suspended in 500 µL of sterile saline to quantify inflammatory cell counts using cell counter.

2.6.4 Estimation of IL-6 CCL2 and IL-1β using ELISA

IL-6, CCL-2and IL-1β protein levels were measured in cell culture-supernatants, BALF and lung tissue homogenates using ELISA kits (R&D Biosystems, Minneapolis, MN, USA) as per the manufacturer's instructions. Briefly, samples along with standards were added into a pre-coated 96 well plate (containing specified capture antibodies) and incubated for 2 hr at room temperature. Then wells were washed with 300 µL of wash buffer thrice, then biotinylated detection antibodies were added and incubated for at room temperature for an hour, followed by incubation with avidin horseradish peroxidase (HRP) conjugate for 30 min. Further, substrate solution was added and incubated in the dark condition for 15 minutes. Subsequently, the reaction was terminated, and the optical density was measured at 450 nm.

2.6.5 Nitric oxide estimation

Nitric oxide estimation was performed as described in our earlier publication (S. K. Tirunavalli et al., 2021). Briefly, cell supernatant (cell culture or tissue homogenates) was collected and used to estimate the NO levels. Griess reagent was used to evaluate the NO levels of the samples by mixing of both supernatants of the lung tissue samples and Griess reagent (1:1 ratio). Then reaction mix was incubated at 37°C for 10 min in dark conditions, and absorbance was measured at 548 nm.

2.6.6 Histopathology and Immunohistochemistry

Histopathology and immunohistochemistry were performed as described earlier (S. K. Tirunavalli et al., 2021). Briefly, a part of the pulmonary lobe was isolated, rinsed with ice-cold PBS, and fixed with 10% neutral-buffered formalin. Paraffin blocks were prepared and sectioned (4 µm) followed by staining with hematoxylin and eosin (H&E) and periodic acid–Schiff (PAS) staining. Few sections were taken on positively charged (Thermofisher USA) slides for immunohistochemistry analysis. The pathological changes in the lungs and alveolitis in lung tissues were scored semi-quantitatively assessed by a pathologist using H&E staining. The scoring system of pathological changes was: 0, no pathologic changes; 1, patchy changes; 2, local changes; 3, scattered changes; 4, severe changes (in most parts of the lung) (Alavinezhad, Hedayati, & Boskabady, 2017). Immunohistochemistry was performed as described in the previous protocol (S. K. Tirunavalli et al., 2021). Briefly, tissue sections were incubated with primary antibodies for 16 hrs. Sections were washed and stained with secondary antibodies. The

protein expression was detected using SignalStain® DAB Chromogen Kit. Neutrophil elastase and MPO protein expressions were semi-quantitatively scored as follows, the highest intensity was graded 'high', the moderate intensity was graded 'medium' and the lowest intensity was graded as 'low'. The intensity was semi-quantitatively converted and plotted as graphs for a better representation of the results.

2.7 Statistical analysis

All experimental results were expressed as mean ± standard error of mean (SEM) and analyzed with the GraphPad Prism 5.0 software. All data were analyzed by one-way or two-way ANOVA with multiple comparisons, where appropriate. In all cases, $P < 0.05$ was considered statistically significant.

3.0 Results

3.1 Characterization of HAEGS

Hydroalcoholic extract of *Gymnema sylvestre* was analysed by LC-ESI-HRMS and MS/MS under both positive and negative ion modes. The resulted mass spectra showed intense $[M+H^+]$ and $[M-H]^-$ ions corresponding to the plant secondary metabolites in positive and negative ion modes, respectively (Table S3-S6). MS data showed possible elemental compositions with mass accuracy of less than ±4.5 **Δ** ppm error. These ions were subjected to MS/MS analysis for further characterization. The resulted MS and MS/MS data was processed through the compound discoverer (version 3.2) using database (Workflow Templates/LC/Natural Product/Natural Product Unknown ID w stats online and Local Database Searches, Reaxys and DNP) and identified a total of 112 metabolites and the majority of these metabolites were derivatives of gymnemic acid, gymnemasaponins, gymnemoside, gymnemasin, and quercetin (Table S3 and S4). In addition, twenty Gymnemic acid analogues and ten flavonoids were manually identified by accurate mass spectral data and presented in Fig. 1A, Fig. S1-S3, Table S5 and Table S6. Similarly, **methanolic extract of** HAEGS was analysed using GC-MS and identified a total of 35 secondary metabolites (Fig. 1B, and Table S7) which include 12 fatty acids (stearic acid, palmitic acid, linolenic acid, octadecenoic acid, stearin, squalene, g-tocopherol), cholesterol, and vitamin E (Fig. 1B, and Table S7). The identified metabolites were corroborated with data base analyzed (For this identification W9N11.L and NIST14 library database were used). Overall, HAEGS is a mixture of several active phyto-molecules.

3.2 HAEGS mitigates the LPS induced cytokine levels in mouse macrophages

Excessive cytokine release is considered to be one of the critical causes of ARDS and multiple-organ failure (Chousterman, Swirski, & Weber, 2017). SARS-CoV-2 induced ARDS exhibited elevated levels of IL-6 in several patients, (Tang et al., 2020b) and it plays key role in disease progression. Before investigating the effect of HAEGS on IL- 6 levels, a cell viability assay was conducted and that results, revealed HAEGS (125 and 250 µg/mL) treatment showed more than 90% cell viability in the presence or absence of LPS (Table. S8). To determine the effect of HAEGS against LPS induced IL-6 release, *in-vitro* assays were performed using RAW-264.7 cells and IL-6 estimation was performed using ELISA. Treatment with LPS (1

µg/mL) significantly increased the IL-6 levels compared to vehicle control, pre-treatment with HAEGS (125, 250, and 500 µg/mL) significantly mitigated the LPS induced IL-6 levels compared to LPS control (Fig. S4 and Table S8). Since it was also reported that, IL-6 is one of the orchestrators for induction of cytokine storm in various inflammatory disorders, next we investigated the effect of HAEGS on other key cytokines and chemokines. To investigate the effect of HAEGS on cytokines and chemokines, RT-qPCR analysis was performed using RAW-264.7 cells upon LPS stimulation. RT-qPCR analysis resulted that LPS induction significantly increased the cytokine, chemokine, and inflammatory marker's expression compared to vehicle control (Fig. 2A-2G). Pre-treatment with HAEGS or dexamethasone (Dexa) reduced the cytokines, chemokines, and inflammatory marker's expression in a dose-dependent manner (Fig. 2A-2G). Taken together, HAEGS significantly ameliorated the LPS induced cytokine expression in dose dependent manner.

3.3 HAEGS mitigates the LPS induced cytokine levels in lung epithelial cells

ARDS is a disease that is result of alveolar epithelial cell injury and pulmonary endothelial cell damage with upregulation of several inflammatory cytokines typically called as cytokine storm (Bachofen & Weibel, 1977). Others and we (Kany, Vollrath, & Relja, 2019; S. K. Tirunavalli et al., 2021) demonstrated that stimulation with LPS (5 µg/mL) significantly increased various cytokines (including IL-6, TNF-α and IL-1β) and lung epithelial cell damage markers in BEAS-2B cells. Similarly, RT-qPCR analysis revealed that LPS stimulation increased the expression of cytokine markers (*IL-6, TNF-α, and IL-1β*) and treatment with HAEGS significantly mitigated the same (Fig. S5A-S5C). Inflammatory markers such as *COX-2* were also increased in LPS stimulation and treatment with HAEGS significantly attenuated (Fig. S5D). Pro-inflammatory chemokines *like IL-8, CCL2, CCL7 and CXCL-11* play a major role in inflammation. To investigate whether the HAEGS protects cells from LPS mediated elevation of chemokines, mRNA expression of various chemokine markers were estimated upon LPS exposure to BEAS-2B cells. mRNA expression analysis revealed that LPS stimulation significantly increased the chemokines expression and pre-treatment with HAEGS reduced the chemokine expression in a dose-dependent manner (Fig. S5E-S5H). HAEGS reduced the chemokine levels better than or equal to dexamethasone. *CC-16* and amphiregulin were reported to be elevated in patients with ventilator-associated lung injury and asthma, it also plays a major role in epithelial cell damage along with adhesion molecules (Determann et al., 2009; Ogata-Suetsugu et al., 2017). Further, RT-qPCR analysis extended to investigate the expression of adhesion molecules and lung epithelial cell damage marker CC-16. Interestingly, HAEGS reduced the LPS induced *CC-16*, amphiregulin, *ICAM, and VCAM* levels along with *CC-16* (Fig. 2H-2K). Overall, HAEGS pre-treatment significantly mitigated the LPS induced cytokine, chemokine, and inflammatory markers expression equivalent to dexamethasone.

3.4 LPS induced ROS levels were abrogated with HAEGS pre-treatment

Reactive oxygen species (ROS) are one of the key signaling molecules that play a substantial role in the progression and maintenance of inflammatory disorders. LPS induces the expression of ROS through multiple mechanisms including the suppression of anti-oxidant enzymes, activation and induction of

NADPH oxidase involved in ROS production (L. Li, Maitra, Singh, & Gan, 2010). Whether HAEGS pre-treatment reduces the levels of NO and ROS levels, we performed nitric oxide estimation and DCFDA measurement assays. Nitric oxide analysis revealed that LPS significantly increased the NO levels in LPS control and pre-treatment with HAEGS significantly reduced the NO levels in mouse macrophages (Fig. S6A). Similar to NO assay, DCFDA assay revealed that, LPS increased the ROS levels in LPS control and treatment with HAEGS or Dexa reduced the ROS levels in a dose-dependent manner (Fig. 3A, 3B and S6B, S6C).

3.5 HAEGS treatment attenuated the cytokine levels by modulating the NF-κB and p38 phosphorylation

Several reports have shown that NF-κB signaling causes the elevated expression of pro-inflammatory genes, including those encoding chemokines and cytokines (Lawrence, 2009). Further, to elucidate the mechanism of action of HAEGS, RAW-264.7 or BEAS-2B cells were pre-treated with HAEGS and further stimulated with LPS. After 12 hr incubation, cells were subjected to Western-blot analysis for elucidation of mechanism. LPS stimulation increased the phospho-p65 and HAEGS treatment significantly reduced the phospho-p65 levels in a dose-dependent manner in both the cell types (Fig. 3C, 3D, 3F, and 3G). MAPK pathway is known to regulate the LPS mediated inflammation in RAW-264.7 cells. Immunoblotting analysis revealed that LPS stimulation increased the phospo-p38 levels, and treatment with HAEGS, same was reduced significantly (Fig. 3C and 3E). Overall, these results demonstrated that HAEGS modulated the NF-κB/MAPK pathway.

3.6 Treatment with HAEGS abrogated the inflammatory cells infiltrations and cytokine storm in rat lungs

Cascade of lung inflammation/injury involves, various inflammatory responses from various cell types including macrophages, immune cells, endothelial and epithelial cells. However, inflammatory cells such as neutrophils, leucocytes or monocytes responds immediately and causes inflammatory cell infiltrations into the effected organs (Turner, Nedjai, Hurst, & Pennington, 2014). In *in-vivo*, several parameters play a major role in inducing the ARDS/lung injury. It was reported that edema occurs as a result of acute lung inflammation leading to increase in lung weight. This could be due to increased infiltration of inflammatory cells because of neutrophil mediated chemotaxis. To investigate the effect of HAEGS against LPS induced ARDS, rat model was employed (Fig. S7). Prior to LPS administration, rats were pre-treated with HAEGS (125 mg/kg and 250 mg/kg) for 2 hr thereafter LPS was administered intratracheally into rats and kept for monitoring. After 24 hr, BALF was collected from rat lungs, then animals were sacrificed, and lungs were isolated. Lung index analysis showed that, LPS alone group showed increased lung weight (wet/dry ratio) compared to sham control, whereas in the treatment group, lung weights were normal, and compared to LPS alone lung weights were significantly reduced (Fig. 4A). Further BALF analysis revealed that neutrophil cell percentage was increased four times in LPS alone group and treatment with HAEGS significantly mitigated the LPS induced infiltration of neutrophils (Fig. 4B). Several studies reported that, neutrophils played a major role in chemotaxis and increased the levels of cytokine/chemokine in lung tissues. RT-qPCR analysis revealed that LPS induced several pro-inflammatory cytokines and chemokines in LPS treated rats compared to sham control lung tissues.

Treatment with HAEGS (125 mg/kg and 250 mg/kg) significantly mitigated the cytokine and chemokine levels (Fig. 4C-4I). These results revealed that pre-treatment with HAEGS significantly ameliorated the LPS induced inflammatory mediators' response in the lungs.

3.7 Treatment with HAEGS mitigated the LPS induced cytokine levels in lung tissues and BALF samples

To validate the BALF analysis and gene expression data, BALF samples and lung tissue samples were subjected to ELISA. IL-6 levels were significantly increased in LPS control group samples (BALF and tissue), whereas in treatment with HAEGS significantly reduced the IL-6 levels (Fig. 5A and 5B). Further investigation was extended to estimate CCL-2, and IL-1b using lung tissue samples. ELISA results revealed that HAEGS treatment significantly reduced the LPS induced elevation of IL-1β and CCL2 levels (Fig. 5C and 5D). Overall, protein expression data validated the gene expression results and it confirmed the protective action of HAEGS against LPS induced cytokine expressions.

3.8 HAEGS ameliorated the LPS induced lung injury by modulating the NF-κB/MAPK pathway

Further, to investigate the possible molecular mechanisms of the anti-inflammatory effect of HAEGS *in-vivo* models, lung tissue samples were subjected to western blot analysis. We have chosen to analyze the expression levels of TNF-α and myeloperoxidase, as these markers are well known to upregulate upon the LPS challenge. HAEGS treatment significantly reduced the LPS induced increase of MPO and TNF-α levels in a dose-dependent manner (Fig. 5E, 5F and 5G). Additionally, we have analyzed the levels of phosphorylated p65, p38, JNK, and ERK, which were significantly increased in LPS control samples compared to sham control. Treatment with HAEGS significantly reduced the phospho-p65, phospho-p38, phospho-ERK, and phosphor-JNK compared to the LPS control tissues (Fig. 5E and 5H-5K). Next, we investigated the effect of HAEGS on MUC5AC, as it is the downstream target of the MAPKinase pathway and is well known to play a vital role in the pathogenesis of airway diseases among other mucins. Western blot analysis revealed that MUC5AC levels were significantly elevated in LPS control samples. Whereas in the HAEGS treated samples, MUC5AC expression levels were showed significantly reduced (Fig. 5E and 5L). Overall, these results indicate that pre-treatment with HAEGS could reverse MPO activation and MUC5AC expression through reduction of phospho-NF-κB expression and phospho-p38 respectively, impeding inflammatory response.

Oxidative stress is the leading cause of various metabolic and non-metabolic diseases, including several types of cancers, and acute lung, kidney and liver inflammations (Arslan et al., 2013; de Lima et al., 2013). Thus, we speculated that HAEGS may perform its role in LPS-induced lung injury by reducing the nitric oxide levels. To prove our hypothesis, lung tissues were subjected to nitric oxide assays and we observed that its levels were significantly elevated in LPS control and the same was reduced in HAEGS pre-treated samples in a dose-dependent manner (Fig. 5M). Taken together, HAEGS treatment suppressed the LPS-induced ALI by inactivating NF-κB/MAPKinase pathway.

3.9 HAEGS treatment protects the LPS induced lung injury and ameliorates the pathological changes

LPS treatment was reported to cause severe damage to the lungs when administered intratracheally into the lungs, which involves induction of interstitial inflammation, edema, and lymphoid infiltration in just 4 hr after its administration (Seemann, Zohles, & Lupp, 2017). To investigate whether HAEGS ameliorates LPS induced pathological changes were reversed with HAEGS or not, lung tissues were subjected to H&E analysis and PAS staining. H&E analysis revealed that LPS induced the elevated interstitial inflammation, infiltration of neutrophils in the alveolar interstitial space, alveolar inflammation, wall thickening, severe edema, peri arteriolar inflammation with infiltration of various inflammatory cells, in LPS control animal lung tissues. Whereas treatment with HAEGS significantly reduced the LPS induced pathological abnormalities in lung tissues (Fig. 6A and 6D). To further confirm that HAEGS could ameliorate the LPS induced lung injury, PAS staining was performed using lung tissue sections. PAS analysis revealed that the percent of PAS-positive goblet cells were remarkably upregulated by LPS instillation, whereas reversed in HAEGS pre-treatment in a dose-dependent manner (Fig. 6B and 6E). The above data demonstrated that HAEGS exhibited a protective role against the LPS-induced ALI in rat models.

3.10 HAEGS ameliorates neutrophil elastase and myeloperoxidase in treated lung tissues

Considering the roles of neutrophil infiltration and its role in inducing the cytokine storm in the lungs, neutrophil elastase levels were investigated in the LPS induced ARDS model. Elevated extracellular release of neutrophil granular enzymes plays a crucial role in causing lung damage. Neutrophil elastase (Ne) degrades the pulmonary ECM proteins and cleaves the respiratory cell-cell adhesion (Yang, Tsai, Pan, & Hwang, 2021). To determine the effect of HAEGS against LPS induced ARDS, lung tissue sections were subjected to immunohistochemistry (IHC) against neutrophil elastase. IHC results revealed that LPS stimulation increased the Ne levels significantly and treatment with HAEGS significantly ameliorated the LPS elevated levels in a dose-dependent manner (Fig. 6C and 6F). Myeloperoxidase (MPO) activity is potentiated by Ne and plays a major role in acute inflammation in the lungs. It was reported that MPO, is an abundant enzyme that is released from neutrophil granules, modulating the course of acute pulmonary inflammatory responses induced by LPS administration. To investigate whether HAEGS mitigates the LPS induced MPO levels in animal model, MPO levels were estimated using immunohistochemistry. IHC results revealed that MPO levels were highly elevated in LPS administered animal's lung tissues, whereas in HAEGS-treated lung tissues these levels were significantly reduced (Fig. 6C and 6G). Overall, these results revealed that HAEGS reduced the LPS induced lung injury and infiltration of inflammatory cells in a dose-dependent manner. In agreement with the results, as shown above, HAEGS displayed a suppressive role in the inflammatory cytokine secretion, suggesting that HAEGS, improved LPS-induced lung injury from cytokine storm-induced inflammation.

3.11 Fraction-6 of HAEGS attenuates the LPS induced pro-inflammatory markers

Since HAEGS is a whole GS leave extract, it contains several types of compounds. To determine the active ingredients which is responsible for therapeutic effect, we used silica column chromatography method to separate various compounds based on their polarity starting with non-polar molecules. About 30 fractions were pooled to six major fractions based on the TLC plate readings (Fig. S8B). All six

fractions were tested for their anti-inflammatory properties along with known main active ingredients of *Gymnema sylvestre* such Gymnemagenin and Deacyl Gymnemic Acid. Interestingly, only fraction 6 (F6) lowered the IL-1β and IL-6 levels in LPS stimulated BEAS-2B cells (Fig. 7A and 7B). To understand the molecular composition of fraction 6, we have carried out different mass spectrometry analysis. A total of 14 metabolites were identified and all metabolites were corresponding to gymnemic acid; deacyl gymnemic acid-II, gymnemic acid-I, IV-X, XIII, XIV, and XVII (Fig. 7C, Fig. S9 and Table 1). Overall, our findings demonstrated that fraction-6 of HAEGS contains components that are active in decreasing ARDS via NF-κB/MAPK pathway regulation of pro-inflammatory marker expression.

Table 1

Identified HAEGS secondary metabolites using LC-HRMS under negative ionization modes in fraction-6

S.No.	Compound name	Chemical formula $[M-H]^-$	Experimental *m/z*	Theoretical *m/z*	Mass error (Δ ppm)	RT (min)
1	Gymnemic acid-I	$C_{43}H_{65}O_{14}$	805.4339	805.4374	-3.70	22.48
2	Deacyl Gymnemic acid-II	$C_{36}H_{57}O_{12}$	681.4183	681.3821	-3.72	19.76
3	Gymnemic acid-IV	$C_{41}H_{63}O_{13}$	763.4232	763.4269	-4.05	21.05
4	Gymnemic acid-V	$C_{46}H_{71}O_{14}$	845.4641	845.4844	-4.87	23.57
5	Gymnemic acid-VI	$C_{47}H_{73}O_{18}$	925.4755	925.4797	-3.39	22.50
6	Gymnemic acid-IX	$C_{47}H_{71}O_{18}$	923.4598	923.4640	-4.19	21.35
7	Gymnemic acid-X	$C_{38}H_{59}O_{13}$	723.3926	723.3956	-3.31	18.75
8	Gymnemic acid-XIII	$C_{41}H_{65}O_{13}$	765.4391	765.4425	-3.79	21.38
9	Gymnemic acid-XIV	$C_{41}H_{63}O_{13}$	763.4232	763.4269	-4.08	20.94
10	Gymnemic acid-XVII	$C_{43}H_{61}O_{13}$	785.4061	785.4112	-3.24	21.29
11	Gymnemagenin	$C_{30}H_{49}O_6$	505.3539	505.3529	3.12	17.56
12	Rutiin	$C_{27}H_{29}O_{16}$	609.1432	609.1456	-2.96	15.50
13	Conduritol	$C_6H_9O_5$	161.04446	161.0450	1.05	14.59
14	Gymnemoside-C	$C_{45}H_{63}O_{14}$	827.4174	827.4218	-4.67	22.71

4.0 Discussion

Various studies have implicated that inflammatory cytokine exert significant effects on the induction and maintenance of inflammatory diseases which require immediate medical attention. Recent pandemic SARC-CoV-2 infection is extremely variable, ranging from no or mild symptoms to severe acute respiratory distress syndrome (Menzella et al., 2020). In several COVID-19 patients, ARDS-induced cytokine storm leads to partial to complete lung damage which results in mortality (Hojyo et al., 2020). Several treatment modalities are practiced in clinics to mitigate the cytokine storm including administration of steroids and cytokine specific monoclonal antibodies. Though, corticosteroids play a prominent role in mitigating the cytokine storm in the early stages of infection, they could cause several side effects due to immune suppression that could lead to even death (Tang et al., 2020a). Tocilizumab treatment showed some promising results in COVID-19 patients with severe respiratory impairment receiving non-invasive mechanical ventilation. However, few patients developed cavitating lung lesions during the follow-up period that implicates that, though tocilizumab treatment is beneficial but could have serious side effects in some patients (Menzella et al., 2020). It was reported that patients with elevated plasma levels of IL-6, IL-8, TNF-α, and IL-1β on day 1 of ARDS had a persistent increase of these inflammatory cytokines over time and led to mortality (Meduri et al., 1995).

In this study, pre-treatment with HAEGS significantly reduced the LPS induced cytokines (*IL-6, IL-1β, TNF-α*), chemokines (*CCL-7, CXCL-8*), inflammatory marker (*COX-2*), and macrophage marker (*F4/80*) expressions in a dose-dependent manner. In numerous lung injury models, the biomarkers *VCAM-1* and *ICAM-1* indicate endothelial damage. (Spadaro et al., 2021). We show that hydroalcoholic extract of the *Gymnema sylvestre* (HAEGS) significantly mitigated the *ICAM-1* and *VCAM*-1 expression in LPS treated lung epithelial cells. It was reported that stimulation of macrophages or epithelial cells with LPS, generates ROS which contributes to the severe inflammation, and leads to elevation of inflammatory markers which may cause damage to the target organs (Liu et al., 2018). Pre-treatment with HAEGS reduced the ROS levels which were gauged by DCFDA analysis and Nitric oxide assay. It has been shown that the activation of NF-κB by LPS treatment is followed by a cascade of events, leading to the activation of several signaling pathways, including PI3K/Akt and MAPKs and that are crucial for regulating inflammation and releasing the inflammatory factors (Jung et al., 2017). Accumulated data suggest that, stimulation of macrophages with LPS leads to activation of MAPK (ERK, JNK, and p38) pathway (van der Bruggen, Nijenhuis, van Raaij, Verhoef, & van Asbeck, 1999). LPS stimulation elevates the phosphorylation of extracellular signal-regulated kinase (ERK) 1/2 and enhances the expression of TNF-α in RAW-264.7 murine macrophages (Shi, Kishore, McMullen, & Nagy, 2002). JNK and p38 (MAPK path way) are mainly activated by bacterial LPS and subsequently by inflammatory cytokines such as TNF-α and IL-1β (Ono & Han, 2000). To determine whether NF-κB and MAPK signaling pathways are involved in the HAEGS-induced inhibition of the inflammatory response, the effects of HAEGS on the activation of the p65, p38, JNK and ERK were investigated. Our results revealed that the LPS-induced phosphorylation of p38, ERK, JNK and p65 were markedly suppressed by pre-treatment with HAEGS. In this study, multiple lines of evidence support that HAEGS pre-treatment significantly attenuated the LPS induced inflammatory cascade in macrophages and lung epithelial cells.

Several studies showed that, after 24 hr of LPS administration, elevated lung wet to dry weight ratio, exuberant infiltration of neutrophils and accumulation of leukocytes, in BALF is an important pathological hallmark of ARDS (Yan Li et al., 2016; Tseng et al., 2012). Neutrophils play a critical role in the initiation, propagation, and resolution of this complex inflammatory environment by infiltrating into the lung and executing a distinct pro-inflammatory function. These include the release of cytokines and reactive oxygen species as well as the production of neutrophil extracellular traps. It has been shown that the number of neutrophils in the BALF of patients with ARDS correlates closely with the severity of the disease (Steinberg et al., 1994), while depletion of polymorphonuclear neutrophils (PMN) in animal models ameliorates lung injury with reduced capillary-alveolar permeability and epithelial cell damage (Abraham, Carmody, Shenkar, & Arcaroli, 2000). In the current study, intratracheal instillation of LPS in rats led to marked increase in lung wet to dry ratio and infiltration of neutrophils in BALF samples. On the other hand, pre-treatment with HAEGS significantly mitigated the same, thus ameliorating lung edema and neutrophil infiltration. Pro-inflammatory chemokines such as *IL-8, CCL2*, and *CCL7* are produced by macrophages or epithelial cells primarily to recruit neutrophils and leukocytes to the affected organs (Turner et al., 2014). Our investigation revealed increase in cytokine and chemokine levels observed in LPS induced control animals is completely mitigated in HAEGS pre-treated rats.

We next, examined the underlying mechanism(s) by which HAEGS mitigates LPS-induced neutrophil infiltration, cytokine expression, elastase expression, myeloperoxidase levels, and lung injury in lung tissues. Our investigation on lung tissue samples revealed that LPS elevated the MPO, TNF-α levels and phosphorylation of p65 and p38, pre-treatment with HAEGS significantly reduced the same in a dose-dependent manner. It was reported that, inhibition or knockdown of p38 or ERK MAPkinase pathway attenuates the cytokine (IL-1β and TNF-α) induced MUC5AC expression in epithelial cells (Song et al., 2003). Similarly, our study also showed that HAEGS pre-treatment reduced the expression of MUC5AC by modulating the pro-inflammatory cytokines and MAPK pathway. The lung histopathological analysis was similar to our previous study (S. K. Tirunavalli et al., 2021), which demonstrated that alveolar septal thickening, interstitial edema, and vascular congestion were elevated in LPS control and all of which was relieved by HAEGS pre-treatment. Further PAS staining results exhibited that, HAEGS rescued the LPS induced upregulation of PAS-positive cells in a dose-dependent manner. Elevated levels of MPO in pulmonary parenchyma, reflecting the activation of neutrophils, was largely over expressed in acute lung injury condition (Dong & Yuan, 2018). Substantial pieces of evidence have confirmed that increased Ne levels are an indispensable contributor to the progression of acute lung injury and its deleterious actions are noticeable in lung tissues (Tsai et al., 2015). Administration of HAEGS significantly reduced both MPO and Ne levels in a dose-dependent manner, suggesting that, HAEGS treatment may ameliorate the neutrophil-mediated damage in lung tissues.

According to characterization studies, the major components in the HAEGS was identified as gymnemic acid, gymnemasaponins, gymnemoside, gymnemasin, quercetin, palmitic acid, stearic acid, linolenic acid, octadecenoic acid, stearin, squalene and γ-tocopherol. Most of these molecules are known for their anti-inflammatory and antioxidant property which directly or indirectly are implicated in the suppression of inflammatory cytokines (Alkhatib & Tuomilehto, 2019). Different derivatives of gymnemasaponins

suppress the glucose uptake indirectly demonstrating the antioxidant property (Yoshikawa, Arihara, & Matsuura, 1991; Yoshikawa, Hirai, Tanaka, & Arihara, 2000). Anti-inflammatory and immune modulating activity has been identified for quercetin in various animal models by reducing visceral adipose tissue, TNF-α and nitric oxide production in addition to downregulating nitric oxide synthase (NOS) production in obese Zucker rats (Rivera, Morón, Sánchez, Zarzuelo, & Galisteo, 2008). γ-tocopherol is known to reduce the oxidative stress in the brain induced by reactive nitrogen species (RNS) (Pahrudin Arrozi et al., 2020). Further, fractionation studies revealed that, only fraction-6 (F6) showed the anti-inflammatory activity among other fractions. Further analysis of the molecular components suggested that F6 contained different derivatives of only gymnemic acid.

Overall, in the current study, we demonstrate that hydroalcoholic extract of *Gymnema sylvestre* strongly attenuates LPS induced cytokines expression, ROS levels in *in-vitro* and *in-vivo* models and PMN infiltration, thus rescuing the rats against LPS-induced ALI. We have further discovered that HAEGS significantly reduces lung injury, MPO, and neutrophil elastase levels by modulating the NF-κB/MAPK pathway. Major active ingredients that are responsible for the observed function are gymnemic acid and its derivatives.

5.0 Conclusion

Cytokine storm/ARDS is a critical phase of viral or bacterial infection of the lungs. Gymnema sylvestre hydroalcoholic extract, which functions as an antioxidant and anti-inflammatory formulation, defends against the cytokine storm in the LPS-induced ARDS model by modulating the NF-κB/MAPK pathway. Either entire HAEGS or fraction 6 (F6) with a gymnemic acid enrichment could be used as a phytochemical medication to treat ARDS and other inflammatory lung injuries.

Abbreviations

ARDS, Acute Respiratory Distress Syndrome; BALF, Bronchoalveolar lavage Fluid (BALF); COVID-19, Coronavirus diseases 2019; CRS, Cytokine Release Syndrome; Dexa, dexamethasone; ERK, extracellular signal-regulated kinase; GC-MS, Gas-Chromatography-Mass spectroscopy; GS, Gymnema sylvestre; HAEGS, JNK, c-Jun N-terminal kinase; hydroalcoholic extract of Gymnema sylvestre; hr, hour; LPS, Lipopolysaccharide, MPO, Myeloperoxidase; NE, Neutrophil elastase; PBS, phosphate buffer saline; ROS, Reactive Oxygen Species; RT-qPCR, Reverse transcriptase quantitative PCR; SRB, Sulforhodamine-B; UHPLC-MS & MS/MS, Ultra performance liquid chromatography-mass spectrometry and Tanden Mass spectrometry.

Declarations

Acknowledgements: Authors thank the Director, CSIR-IICT, Hyderabad, India, for providing facilities and funding necessary for the conducting of this work. AJ thank the Council of Scientific and Industrial Research (CSIR), New Delhi, India, for the award of Research associate (RA) and SKT thank the ICMR,

New Delhi, India for the award of senior research fellow (SRF). CSIR-IICT manuscript communication number: IICT/Pubs./2021/386.

Funding: Used internal funds of the CSIR-Indian Institute of Chemical Technology, Hyderabad. This research did not receive any specific grant from funding agencies in the public, commercial, or not-for-profit sectors.

Competing interests

The authors declare no competing or financial interests.

Author contributions

Conceptualization: A.A. and S.B.A; Methodology: A.J, TSK, S.B.A, A.A; Preparation and analysis of extract: B.M.A, B. K, Analysis of extract: S. S.P, J. R. T:, Validation: AA, S.B.A, ; Invitro cell culture: AJ and SKT. RT-qPCR, Western-blot analysis, ex-vivo and *in-vivo* experiments: A.J., TSK, Immunohistochemistry analysis: A.J and TSK. Pathological studies: E. J, Manuscript writing - review & editing: S.B.A, A.A.; funding acquisition: A.A and S.B.A.

References

1. Abraham, E., Carmody, A., Shenkar, R., & Arcaroli, J. (2000). Neutrophils as early immunologic effectors in hemorrhage- or endotoxemia-induced acute lung injury. *Am J Physiol Lung Cell Mol Physiol, 279*(6), L1137-1145. doi:10.1152/ajplung.2000.279.6.L1137
2. Alavinezhad, A., Hedayati, M., & Boskabady, M. H. (2017). The effect of Zataria multiflora and carvacrol on wheezing, FEV1 and plasma levels of nitrite in asthmatic patients. *Avicenna journal of phytomedicine, 7*(6), 531-541.
3. Aleisa, A. M., Al-Rejaie, S. S., Abuohashish, H. M., Ola, M. S., Parmar, M. Y., & Ahmed, M. M. (2014). Pretreatment of Gymnema sylvestre revealed the protection against acetic acid-induced ulcerative colitis in rats. *BMC Complementary and Alternative Medicine, 14*(1), 49. doi:10.1186/1472-6882-14-49
4. Alkhatib, A., & Tuomilehto, J. J. E. o. E. D. (2019). Lifestyle Diabetes Prevention.
5. Andugulapati, S. B., Gourishetti, K., Tirunavalli, S. K., Shaikh, T. B., & Sistla, R. (2020). Biochanin-A ameliorates pulmonary fibrosis by suppressing the TGF-β mediated EMT, myofibroblasts differentiation and collagen deposition in in vitro and in vivo systems. *Phytomedicine, 78*, 153298. doi:https://doi.org/10.1016/j.phymed.2020.153298
6. Arslan, F., Lai, R. C., Smeets, M. B., Akeroyd, L., Choo, A., Aguor, E. N., . . . de Kleijn, D. P. (2013). Mesenchymal stem cell-derived exosomes increase ATP levels, decrease oxidative stress and activate PI3K/Akt pathway to enhance myocardial viability and prevent adverse remodeling after myocardial ischemia/reperfusion injury. *Stem Cell Res, 10*(3), 301-312. doi:10.1016/j.scr.2013.01.002

7. Aslan, A., Aslan, C., Zolbanin, N. M., & Jafari, R. (2021). Acute respiratory distress syndrome in COVID-19: possible mechanisms and therapeutic management. *Pneumonia, 13*(1), 14. doi:10.1186/s41479-021-00092-9
8. Bachofen, M., & Weibel, E. R. (1977). Alterations of the gas exchange apparatus in adult respiratory insufficiency associated with septicemia. *Am Rev Respir Dis, 116*(4), 589-615. doi:10.1164/arrd.1977.116.4.589
9. Barnes, P. J., & Adcock, I. (1993). Anti-inflammatory actions of steroids: molecular mechanisms. *Trends Pharmacol Sci, 14*(12), 436-441. doi:10.1016/0165-6147(93)90184-l
10. Baskaran, K., Kizar Ahamath, B., Radha Shanmugasundaram, K., & Shanmugasundaram, E. R. (1990). Antidiabetic effect of a leaf extract from Gymnema sylvestre in non-insulin-dependent diabetes mellitus patients. *J Ethnopharmacol, 30*(3), 295-300. doi:10.1016/0378-8741(90)90108-6
11. Chousterman, B. G., Swirski, F. K., & Weber, G. F. (2017). Cytokine storm and sepsis disease pathogenesis. *Semin Immunopathol, 39*(5), 517-528. doi:10.1007/s00281-017-0639-8
12. Dadinaboyina, S. B., Yerra, N. V., Adimoolam, B. M., Parsa, S., Bathini, N. B., & Thota, J. R. (2021). Identification and characterization of degradation products of Remdesivir using liquid chromatography/mass spectrometry. *New Journal of Chemistry, 45*(16), 7217-7224. doi:10.1039/D1NJ00160D
13. de Lima, F. M., Albertini, R., Dantas, Y., Maia-Filho, A. L., Santana Cde, L., Castro-Faria-Neto, H. C., . . . Aimbire, F. (2013). Low-level laser therapy restores the oxidative stress balance in acute lung injury induced by gut ischemia and reperfusion. *Photochem Photobiol, 89*(1), 179-188. doi:10.1111/j.1751-1097.2012.01214.x
14. Determann, R. M., Millo, J. L., Waddy, S., Lutter, R., Garrard, C. S., & Schultz, M. J. (2009). Plasma CC16 levels are associated with development of ALI/ARDS in patients with ventilator-associated pneumonia: a retrospective observational study. *BMC pulmonary medicine, 9*, 49-49. doi:10.1186/1471-2466-9-49
15. Dong, Z., & Yuan, Y. (2018). Accelerated inflammation and oxidative stress induced by LPS in acute lung injury: Inhibition by ST1926. *International Journal of Molecular Medicine, 41*. doi:10.3892/ijmm.2018.3574
16. Hojyo, S., Uchida, M., Tanaka, K., Hasebe, R., Tanaka, Y., Murakami, M., & Hirano, T. (2020). How COVID-19 induces cytokine storm with high mortality. *Inflammation and regeneration, 40*, 37-37. doi:10.1186/s41232-020-00146-3
17. Jung, J.-S., Choi, M.-J., Lee, Y. Y., Moon, B.-I., Park, J.-S., & Kim, H.-S. (2017). Suppression of Lipopolysaccharide-Induced Neuroinflammation by Morin via MAPK, PI3K/Akt, and PKA/HO-1 Signaling Pathway Modulation. *Journal of Agricultural and Food Chemistry, 65*(2), 373-382. doi:10.1021/acs.jafc.6b05147
18. Kanetkar, P., Singhal, R., & Kamat, M. (2007). Gymnema sylvestre: A Memoir. *Journal of clinical biochemistry and nutrition, 41*(2), 77-81. doi:10.3164/jcbn.2007010

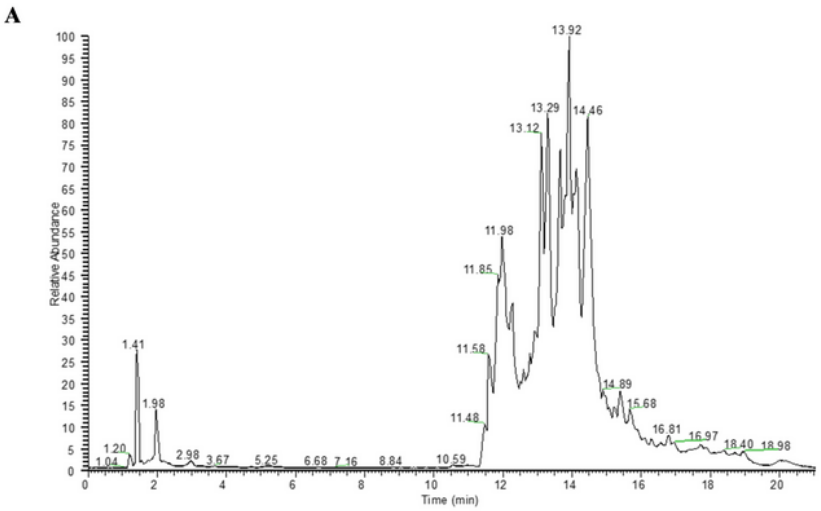
19. Kanetkar, P., Singhal, R., & Kamat, M. (2007). Gymnema sylvestre: A Memoir. *J Clin Biochem Nutr, 41*(2), 77-81. doi:10.3164/jcbn.2007010
20. Kany, S., Vollrath, J. T., & Relja, B. (2019). Cytokines in Inflammatory Disease. *International journal of molecular sciences, 20*(23), 6008. doi:10.3390/ijms20236008
21. Khiali, S., Khani, E., & Entezari-Maleki, T. (2020). A Comprehensive Review of Tocilizumab in COVID-19 Acute Respiratory Distress Syndrome. *60*(9), 1131-1146. doi:https://doi.org/10.1002/jcph.1693
22. Lawrence, T. (2009). The nuclear factor NF-kappaB pathway in inflammation. *Cold Spring Harb Perspect Biol, 1*(6), a001651. doi:10.1101/cshperspect.a001651
23. Leach, M. J. (2007). Gymnema sylvestre for diabetes mellitus: a systematic review. *J Altern Complement Med, 13*(9), 977-983. doi:10.1089/acm.2006.6387
24. Li, L., Maitra, U., Singh, N., & Gan, L. (2010). Molecular mechanism underlying LPS-induced generation of reactive oxygen species in macrophages. *24*(S1), 422.423-422.423. doi:https://doi.org/10.1096/fasebj.24.1_supplement.422.3
25. Li, Y., Huang, J., Foley, N. M., Xu, Y., Li, Y. P., Pan, J., . . . Wang, J. (2016). B7H3 ameliorates LPS-induced acute lung injury via attenuation of neutrophil migration and infiltration. *Scientific Reports, 6*(1), 31284. doi:10.1038/srep31284
26. Li, Y., Xiao, Y., Gao, W., Pan, J., Zhao, Q., & Zhang, Z. (2019). Gymnemic acid alleviates inflammation and insulin resistance via PPARδ- and NFκB-mediated pathways in db/db mice. *Food & Function, 10*(9), 5853-5862. doi:10.1039/C9FO01419E
27. Li, Y., Yao, J., Han, C., Yang, J., Chaudhry, M. T., Wang, S., . . . Yin, Y. (2016). Quercetin, Inflammation and Immunity. *8*(3), 167.
28. Liu, Z., Ren, Z., Zhang, J., Chuang, C.-C., Kandaswamy, E., Zhou, T., & Zuo, L. J. F. i. p. (2018). Role of ROS and nutritional antioxidants in human diseases. *9*, 477.
29. Malik, J., Manvi, F., Alagawadi, K., & Noolvi, M. J. I. j. o. g. p. (2008). Evaluation of anti-inflammatory activity of Gymnema sylvestre leaves extract in rats. *2*(2), 114.
30. Manicone, A. M. (2009). Role of the pulmonary epithelium and inflammatory signals in acute lung injury. *Expert review of clinical immunology, 5*(1), 63-75. doi:10.1586/177666X.5.1.63
31. Meduri, G. U., Headley, S., Kohler, G., Stentz, F., Tolley, E., Umberger, R., & Leeper, K. (1995). Persistent elevation of inflammatory cytokines predicts a poor outcome in ARDS. Plasma IL-1 beta and IL-6 levels are consistent and efficient predictors of outcome over time. *Chest, 107*(4), 1062-1073. doi:10.1378/chest.107.4.1062
32. Menzella, F., Fontana, M., Salvarani, C., Massari, M., Ruggiero, P., Scelfo, C., . . . Facciolongo, N. (2020). Efficacy of tocilizumab in patients with COVID-19 ARDS undergoing noninvasive ventilation. *Critical Care, 24*(1), 589. doi:10.1186/s13054-020-03306-6
33. Merad, M., & Martin, J. C. (2020). Pathological inflammation in patients with COVID-19: a key role for monocytes and macrophages. *Nature Reviews Immunology, 20*(6), 355-362. doi:10.1038/s41577-020-0331-4

34. Ogata-Suetsugu, S., Yanagihara, T., Hamada, N., Ikeda-Harada, C., Yokoyama, T., Suzuki, K., . . . Nakanishi, Y. (2017). Amphiregulin suppresses epithelial cell apoptosis in lipopolysaccharide-induced lung injury in mice. *Biochem Biophys Res Commun, 484*(2), 422-428. doi:10.1016/j.bbrc.2017.01.142
35. Ono, K., & Han, J. (2000). The p38 signal transduction pathway: activation and function. *Cell Signal, 12*(1), 1-13. doi:10.1016/s0898-6568(99)00071-6
36. Pahrudin Arrozi, A., Shukri, S. N. S., Wan Ngah, W. Z., Mohd Yusof, Y. A., Ahmad Damanhuri, M. H., Jaafar, F., & Makpol, S. (2020). Comparative Effects of Alpha- and Gamma-Tocopherol on Mitochondrial Functions in Alzheimer's Disease In Vitro Model. *Scientific Reports, 10*(1), 8962. doi:10.1038/s41598-020-65570-4
37. Rivera, L., Morón, R., Sánchez, M., Zarzuelo, A., & Galisteo, M. (2008). Quercetin ameliorates metabolic syndrome and improves the inflammatory status in obese Zucker rats. *Obesity (Silver Spring), 16*(9), 2081-2087. doi:10.1038/oby.2008.315
38. Sahu, N. P., Mahato, S. B., Sarkar, S. K., & Poddar, G. (1996). Triterpenoid saponins from Gymnema sylvestre. *Phytochemistry, 41*(4), 1181-1185. doi:10.1016/0031-9422(95)00782-2
39. Seemann, S., Zohles, F., & Lupp, A. (2017). Comprehensive comparison of three different animal models for systemic inflammation. *Journal of Biomedical Science, 24*(1), 60. doi:10.1186/s12929-017-0370-8
40. Shi, L., Kishore, R., McMullen, M. R., & Nagy, L. E. (2002). Lipopolysaccharide stimulation of ERK1/2 increases TNF-α production via Egr-1. *282*(6), C1205-C1211. doi:10.1152/ajpcell.00511.2001
41. Song, K. S., Lee, W. J., Chung, K. C., Koo, J. S., Yang, E. J., Choi, J. Y., & Yoon, J. H. (2003). Interleukin-1 beta and tumor necrosis factor-alpha induce MUC5AC overexpression through a mechanism involving ERK/p38 mitogen-activated protein kinases-MSK1-CREB activation in human airway epithelial cells. *J Biol Chem, 278*(26), 23243-23250. doi:10.1074/jbc.M300096200
42. Spadaro, S., Fogagnolo, A., Campo, G., Zucchetti, O., Verri, M., Ottaviani, I., . . . Contoli, M. (2021). Markers of endothelial and epithelial pulmonary injury in mechanically ventilated COVID-19 ICU patients. *Critical Care, 25*(1), 74. doi:10.1186/s13054-021-03499-4
43. Spagnolo, P., Balestro, E., Aliberti, S., Cocconcelli, E., Biondini, D., Casa, G. D., . . . Maher, T. M. (2020). Pulmonary fibrosis secondary to COVID-19: a call to arms? *Lancet Respir Med, 8*(8), 750-752. doi:10.1016/s2213-2600(20)30222-8
44. Steinberg, K. P., Milberg, J. A., Martin, T. R., Maunder, R. J., Cockrill, B. A., & Hudson, L. D. (1994). Evolution of bronchoalveolar cell populations in the adult respiratory distress syndrome. *Am J Respir Crit Care Med, 150*(1), 113-122. doi:10.1164/ajrccm.150.1.8025736
45. Subramani, S. K., Gupta, Y., Manish, M., & Prasad, G. (2020). Gymnema Sylvestre A- Potential Inhibitor of COVID-19 Main Protease by MD Simulation Study. In: ChemRxiv.
46. Takeuchi, O., & Akira, S. (2010). Pattern recognition receptors and inflammation. *Cell, 140*(6), 805-820. doi:10.1016/j.cell.2010.01.022

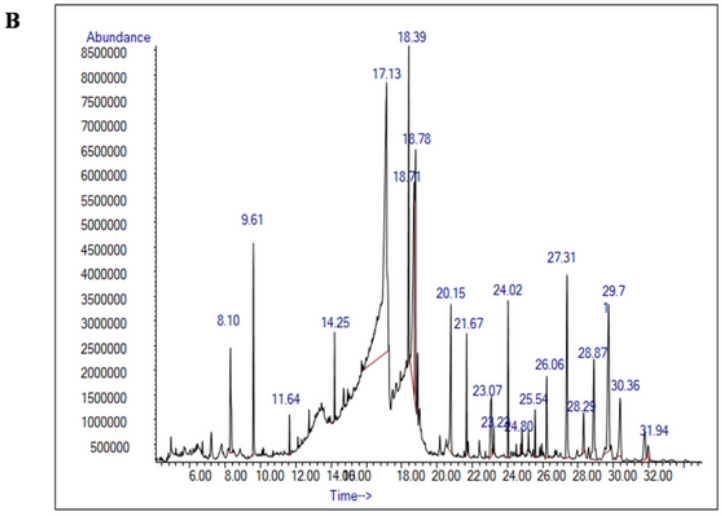
47. Tang, Y., Liu, J., Zhang, D., Xu, Z., Ji, J., & Wen, C. (2020a). Cytokine Storm in COVID-19: The Current Evidence and Treatment Strategies. *Frontiers in immunology, 11*, 1708-1708. doi:10.3389/fimmu.2020.01708
48. Tang, Y., Liu, J., Zhang, D., Xu, Z., Ji, J., & Wen, C. (2020b). Cytokine Storm in COVID-19: The Current Evidence and Treatment Strategies. *11*. doi:10.3389/fimmu.2020.01708
49. Tirunavalli, S. K., Gourishetti, K., Kotipalli, R. S. S., Kuncha, M., Kathirvel, M., Kaur, R., . . . Andugulapati, S. B. (2021). Dehydrozingerone ameliorates Lipopolysaccharide induced acute respiratory distress syndrome by inhibiting cytokine storm, oxidative stress via modulating the MAPK/NF-κB pathway. *Phytomedicine, 92*, 153729. doi:10.1016/j.phymed.2021.153729
50. Tirunavalli, S. K., Gourishetti, K., Kotipalli, R. S. S., Kuncha, M., Kathirvel, M., Kaur, R., . . . Andugulapati, S. B. (2021). Dehydrozingerone ameliorates Lipopolysaccharide induced acute respiratory distress syndrome by inhibiting cytokine storm, oxidative stress via modulating the MAPK/NF-κB pathway. *Phytomedicine, 92*, 153729-153729. doi:10.1016/j.phymed.2021.153729
51. Tiwari, P., Mishra, B. N., & Sangwan, N. S. (2014). Phytochemical and pharmacological properties of Gymnema sylvestre: an important medicinal plant. *BioMed research international, 2014*, 830285-830285. doi:10.1155/2014/830285
52. Tiwari, P., Mishra, B. N., & Sangwan, N. S. (2014). Phytochemical and pharmacological properties of Gymnema sylvestre: an important medicinal plant. *Biomed Res Int, 2014*, 830285. doi:10.1155/2014/830285
53. Tsai, Y.-F., Yu, H.-P., Chang, W.-Y., Liu, F.-C., Huang, Z.-C., & Hwang, T.-L. (2015). Sirtinol Inhibits Neutrophil Elastase Activity and Attenuates Lipopolysaccharide-Mediated Acute Lung Injury in Mice. *Scientific Reports, 5*(1), 8347. doi:10.1038/srep08347
54. Tseng, T.-L., Chen, M.-F., Tsai, M.-J., Hsu, Y.-H., Chen, C.-P., & Lee, T. J. F. (2012). Oroxylin-A rescues LPS-induced acute lung injury via regulation of NF-κB signaling pathway in rodents. *PloS one, 7*(10), e47403-e47403. doi:10.1371/jsournal.pone.0047403
55. Turner, M. D., Nedjai, B., Hurst, T., & Pennington, D. J. (2014). Cytokines and chemokines: At the crossroads of cell signalling and inflammatory disease. *Biochimica et Biophysica Acta (BBA) - Molecular Cell Research, 1843*(11), 2563-2582. doi:https://doi.org/10.1016/j.bbamcr.2014.05.014
56. van der Bruggen, T., Nijenhuis, S., van Raaij, E., Verhoef, J., & van Asbeck, B. S. (1999). Lipopolysaccharide-induced tumor necrosis factor alpha production by human monocytes involves the raf-1/MEK1-MEK2/ERK1-ERK2 pathway. *Infect Immun, 67*(8), 3824-3829. doi:10.1128/iai.67.8.3824-3829.1999
57. Yang, S.-C., Tsai, Y.-F., Pan, Y.-L., & Hwang, T.-L. (2021). Understanding the role of neutrophils in acute respiratory distress syndrome. *Biomedical Journal, 44*(4), 439-446. doi:https://doi.org/10.1016/j.bj.2020.09.001
58. Yoshikawa, K., Arihara, S., & Matsuura, K. (1991). A new type of antisweet principles occurring in Gymnema sylvestre. *Tetrahedron Letters, 32*(6), 789-792. doi:https://doi.org/10.1016/S0040-4039(00)74887-8

59. Yoshikawa, K., Hirai, H., Tanaka, M., & Arihara, S. (2000). Antisweet Natural Products. XV. Structures of Jegosaponins A-D from Styrax japonica SIEB. et ZUCC. *CHEMICAL & PHARMACEUTICAL BULLETIN, 48*(7), 1093-1096. doi:10.1248/cpb.48.1093

Figures



UHPLC-ESI-Orbitrap Total ion chromatogram of HAEGS.



Total ion chromatogram (GC-MS) of HAEGS.

Fig.1

Figure 1

Chromatographic and GC analysis of HAEGS

1A: Chromatographic separations of *Gymnema sylvestre* plant extract was carried out on a Surveyor UHPLC system using an Syncronis C18 column (2.1 × 100 mm) column with a gradient mobile phase of acetonitrile and 0.1% formic acid in water with a flow rate of 0.15 mL min^{-1}. In the LC-HRMS analysis, a total of 20 plant secondary metabolites were identified based on the derived elemental compositions from the high-resolution mass spectral data. Thermo Xcalibur software (version 2.2) was used for processing the mass spectral data.

1B: The GC analysis was performed with Agilent 6890 GC equipped with Agilent Technologies5977A mass selective detector (MSD). The separation of analytes was carried out on Capillary Column (Agilent) HP-5% Phenyl Methyl Siloxane (30mx250umx0.5um). The volatile organic compounds were identified by using the W9N11.L, NIST14 library database. In this analysis, a total of 19 plant secondary metabolites were identified Mass spectral data was processed using MSD ChemStation.

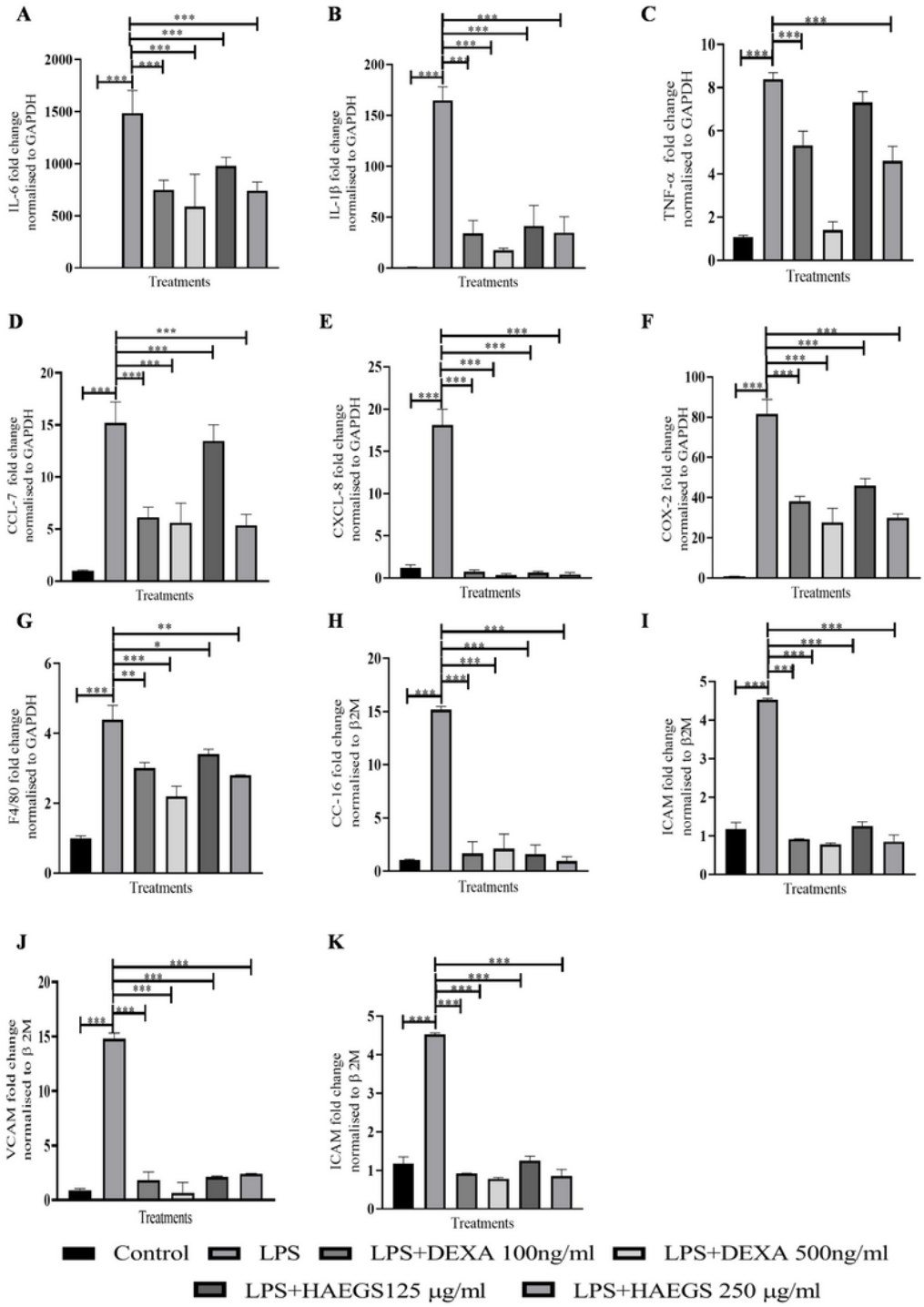


Fig.2

Figure 2

HAEGS treatment mitigates the LPS induced gene expression in RAW 264.7 and epithelial cells

A-G) RAW-264.7 cells were cultured in serum free media for 6 h, then cells were pre-treated with HAEGS (125 and 250 µg/mL) or Dexamethasone (100 ng/mL and 500 ng/mL), for a period of 2hr, then cells were stimulated with LPS (1 µg/mL) for a period of 12 hr. H-K) BEAS-2B cells were pre-treated with HAEGS

(125 and 250 µg/mL) or DEXA (100 ng/mL and 500 ng/mL) for 2hr, further, cells were stimulated with LPS (5 µg/mL) for another 12hr. Thereafter, cells were subjected to qRT-PCR analysis using specified primer sets. Graphs in panels represent fold change in gene expression normalized to β2M. * $p < 0.05$, ** $p < 0.01$, *** $p < 0.001$. NS, non-significant. One way ANOVA was performed for statistical analysis. Data represented as Mean ± SEM, n = 3.

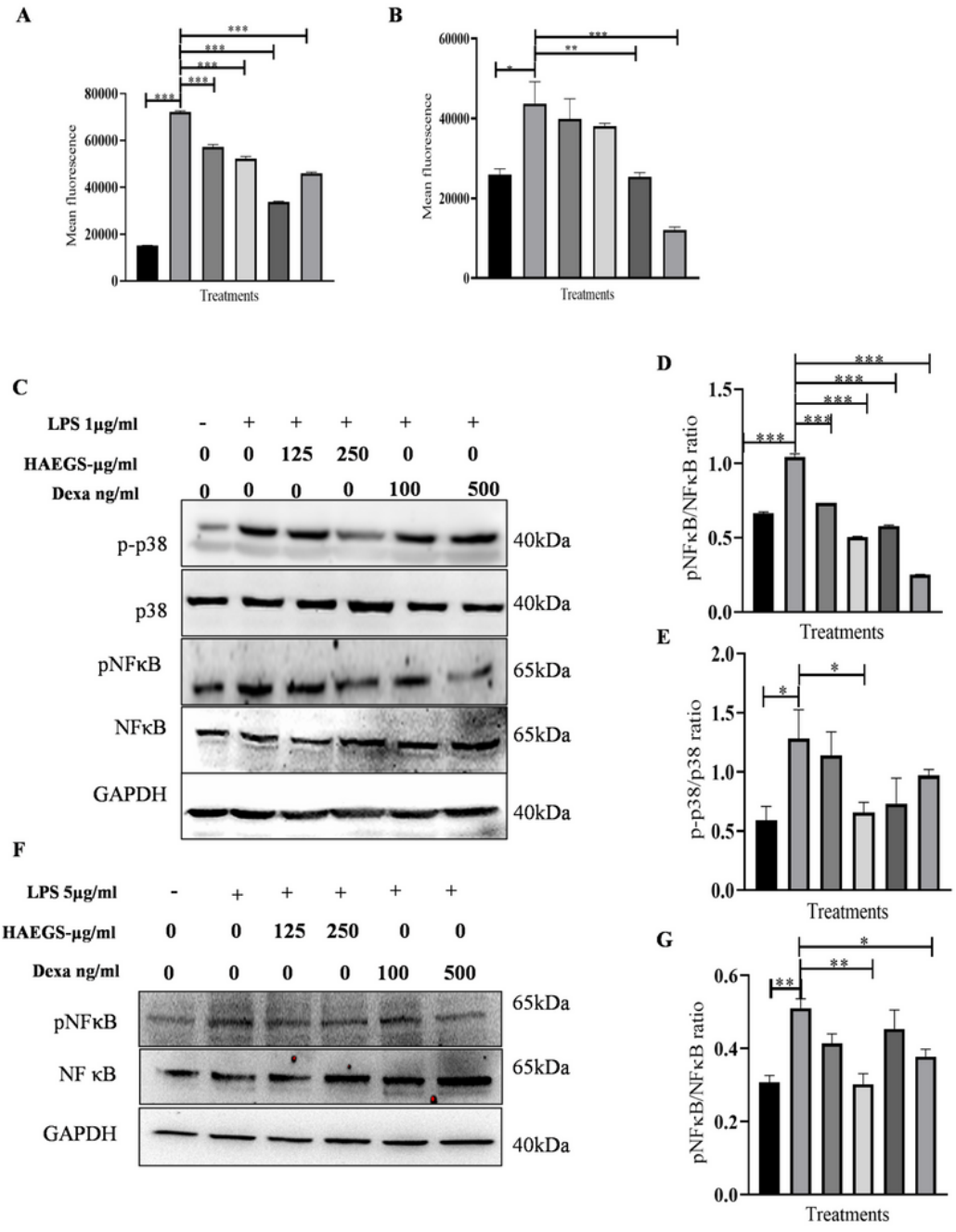


Fig.3

Figure 3

HAEGS ameliorates the inflammatory mediators by mitigating the oxidative stress and modulating the MAPK and NF-κB pathways.

A-B) RAW-264.7 (A) or BEAS-2B (B) cells were pre-treated with HAEGS (125 and 250 µg/mL) or DEXA (100 ng/mL and 500 ng/mL) for 2hr, then cells were stimulated with LPS (1 µg/mL or 5 µg/mL) or for another 12 hr. Thereafter, cells were trypsinized and subjected to DCFDA analysis using flow-cytometry. **C-G)** RAW-264.7 (C-E) or BEAS-2B (F-G) cells were pre-treated with HAEGS (125 and 250 µg/mL) and DEXA (100 ng/mL and 500 ng/mL) after 2 hr, cells were stimulated with LPS (1 µg/mL) for another 12 hr. Further, cells were subjected to western-blot analysis using specified antibodies. Protein expressions were quantified using image J software and graphs were plotted against each specified protein markers.

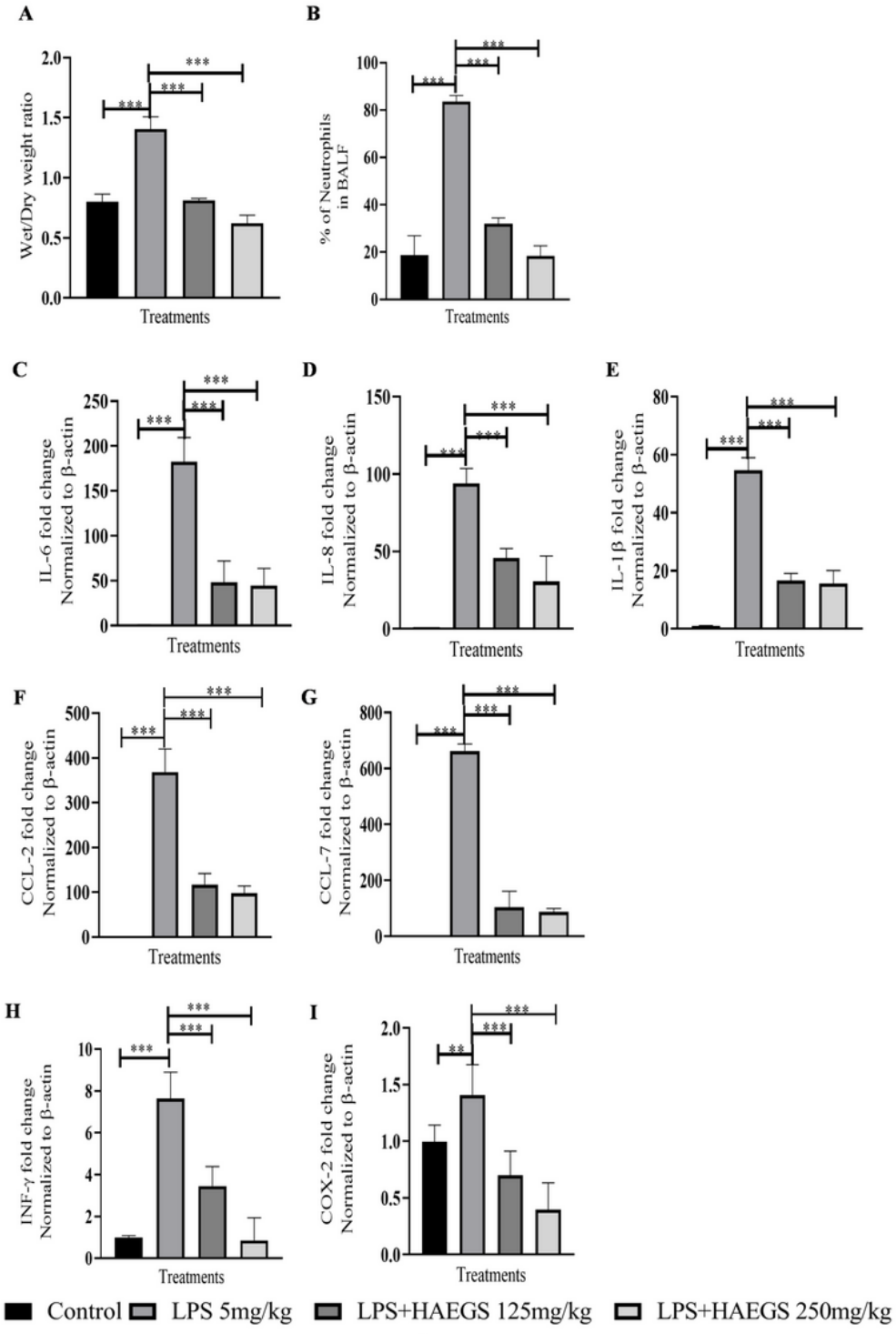


Fig.4

Figure 4

Pre-treatment with HAEGS reducing the LPS induced physiological changes and inflammatory responses in rat lungs.

ARDS model was developed in male SD rats by intra-tracheal instillation of LPS (5 mg/kg). Post pre-treatment, rats were challenged with LPS 5 mg/kg and then kept for 24hr monitoring. Thereafter, rats

were anesthetized and BALF fluid was collected from 4 rats for cell counting and lung tissue were collected from another four animals for estimating the dry/wet ratio and qRT-PCR analysis for the specified primers. **A, B)** Shows the effect of HAEGS against lipopolysaccharide (LPS) induced elevation of lung wet to dry ratio (A) and neutrophils infiltration in Bronchiolar Lavage Fluid (B). **C-I)** Represents the mRNA expression of various inflammatory markers in rat lung tissues.

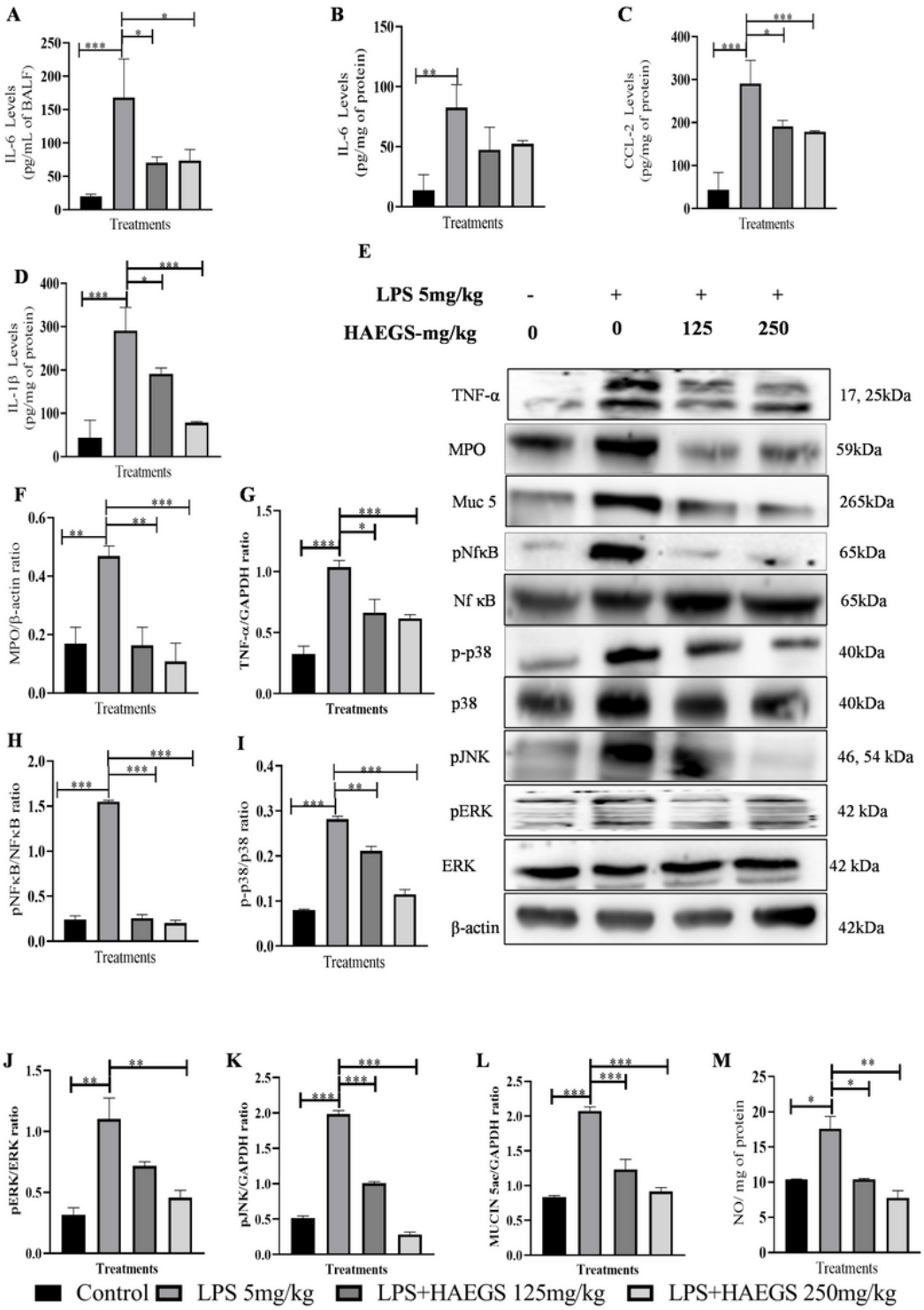


Fig.5

Figure 5

HAEGS abrogated the inflammatory cytokines in LPS stimulated lung tissue homogenates by reducing the oxidative stress and modulating the NF-κB pathway

After 24 hr of treatment, lung tissues were collected and part of BALF (A) and tissue samples (B-D) were subjected for ELISA for the specified protein estimations (A–D). After treatment period, lung tissues were collected, and part of tissues were homogenized and subjected to immunoblot analysis for the specified antibodies and part of the tissues were subjected to nitic oxide analysis. E) Representative images of western blot. (F–L) Graph represents densitometric quantification of the specified proteins; Nitric oxide estimation (M). * $p < 0.05$; ** $p < 0.01$; *** $p < 0.001$ vs. the LPS control group. Data represented as Mean ± SEM, n = 8. One way ANOVA was performed for statistical analysis.

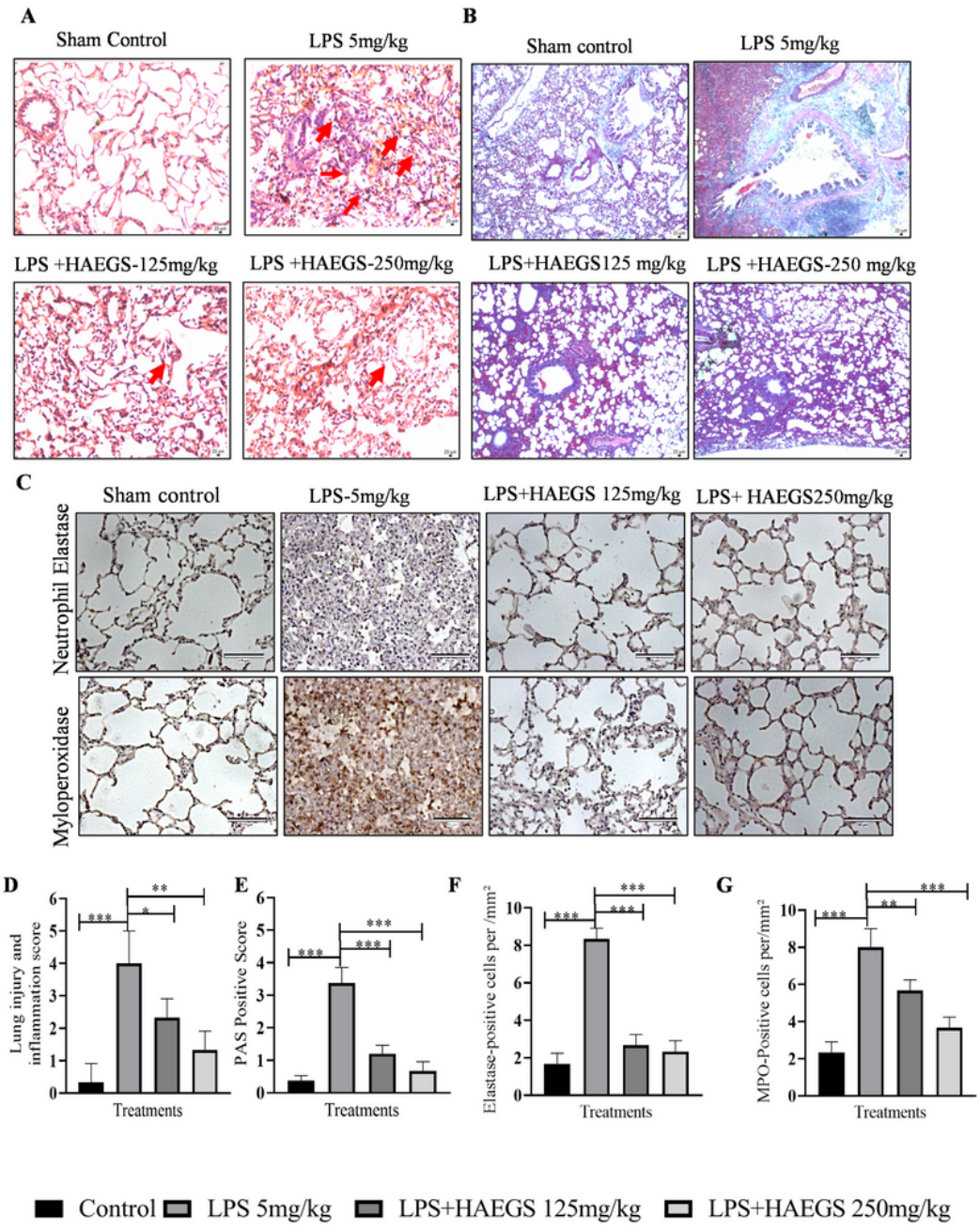


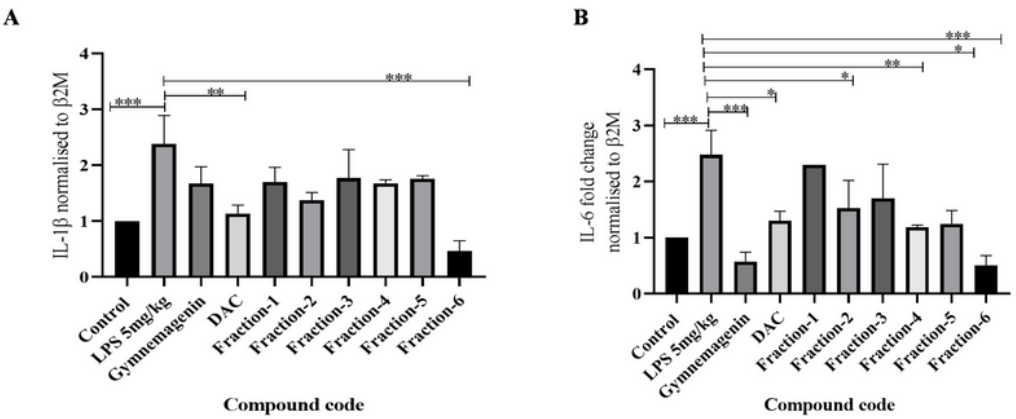
Fig.6

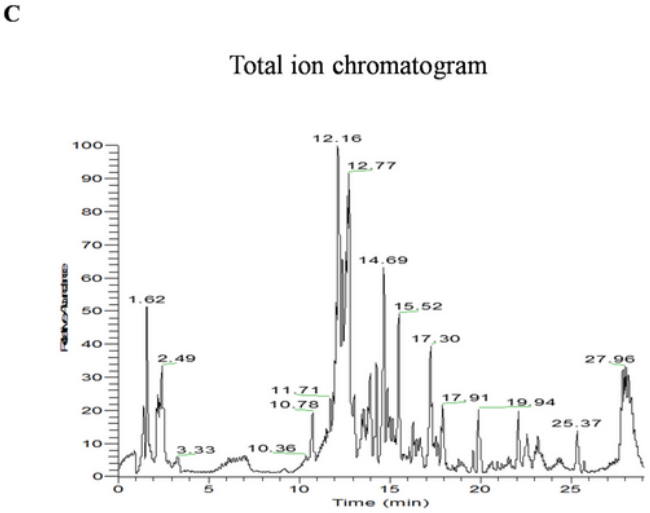
Figure 6

HAEGS treatment ameliorates the infiltration of inflammatory cells, pathological changes and Neutrophil mediated events in LPS stimulated lung tissues.

After treatment period, lungs were subjected to histopathology. (A) Representative images (10×) of H&E-staining, the red arrow points at typical areas of inflammation, manifesting oedema and infiltration of

inflammatory cells. Graphs represent the score of (D) lung injury and inflammation score. PAS staining was used to observe goblet cells in LPS-induced mice with acute lung injury. (B) Representative images (10x) of PAS staining. Goblet cells were identified using PAS in LPS-induced rat lungs. (E) The quantification of PAS-positive score**.** C, F and G) Immunohistochemistry of Myeloperoxidase images and Neutrophil elastase images (C) quantification of Neutrophil elastase (F) quantification of MPO (G) in the lung sections. Images were taken under original magnification × 20. n = 8 * $p < 0.05$; ** $p < 0.01$; *** $p < 0.001$ vs. the LPS control group. Data represented as Mean ± SEM. One way ANOVA was performed for statistical analysis.





Identified GS plant secondary metabolites using LC-HRMS under Negative ionization mode-Fraction-6

Fig.7

Figure 7

Fraction 6 metabolites significantly inhibited the IL-6 and IL-1β in BEAS-2B cells

A) Fraction 6 of HAEGS chromatographic separations were carried out on a Surveyor UHPLC system using an Syncronis C18 column (2.1 × 100 mm; Thermo scientific, Germany) column with a gradient mobile phase of 0.1% formic acid in water and acetonitrile with a flow rate of 0.15 mL min^{-}. B and C)

HAEGS was fractionated using column chromatography and BEAS-2B cells were cultured in serum free media for 6 hr, then cells were pre-treated with various fractions of HAEGS (25µg/mL) or Deacyl gymnemic acid or Gymnemagenin or (100 µg/mL), for a period of 2 hr, then cells were stimulated with LPS (5 µg/mL) for a period of 12 hr. Thereafter, cells were subjected to qRT-PCR analysis using specified primer sets. Graphs in panels represent fold change in gene expression normalized to β2M. * $p < 0.05$, ** $p < 0.01$, *** $p < 0.001$. NS, non-significant. One way ANOVA was performed for statistical analysis. Data represented as Mean ± SEM, n = 3.

Supplementary Files

This is a list of supplementary files associated with this preprint. Click to download.

- Fig.S1.tif
- Fig.S2.tif
- Fig.S3.tif
- Fig.S4.tif
- Fig.S5.tif
- Fig.S6.tif
- Fig.S7.tif
- Fig.S8.tif
- Fig.S9.tif
- Fig.S10.tif
- Fig.S11.tif
- SupplementaryTables1.docx
- Supplementaryfigurelegends.docx